

Classical inflaton field induced creation of superheavy dark matter

Daniel J. H. Chung*

*Department of Physics and Enrico Fermi Institute
The University of Chicago, Chicago, Illinois 60637, and
NASA/Fermilab Astrophysics Center
Fermi National Accelerator Laboratory, Batavia, Illinois 60510*

We calculate analytically and numerically the production of superheavy dark matter (X) when it is coupled to the inflaton field ϕ within the context of a slow-roll $m_\phi^2\phi^2/2$ inflationary model with coupling $g^2X^2\phi^2/2$. We find that X particles with a mass as large as $1000 H_i$, where H_i is the value of the Hubble expansion rate at the end of inflation, can be produced in sufficient abundance to be cosmologically significant today. This means that superheavy dark matter may have a mass of up to $10^{-3}M_{\text{Pl}}$. We also derive a simple formula that can be used to estimate particle production as a result of a quantum field's interaction with a general class of homogeneous classical fields. Finally, we note that the combined effect of the inflaton field and the gravitational field on the X field causes the production to be a nonmonotonic function of g^2 .

PACS number(s): 98.80.Cq, 4.62.+v, 95.35.+d

*Electronic mail: djchung@feynman.physics.lsa.umich.edu

I. INTRODUCTION

The rotation curves deduced from observing luminous matter (see for example [1]) indicate dark matter (DM) exists around galaxies. Furthermore, comparison of the peculiar velocities of many galaxies with the detailed maps of density contrast suggest [2] that $\Omega > 0.3$. However, these cannot be all in the form of baryons according to the standard scenarios of big bang nucleosynthesis [3, 4]. Structure formation studies indicate that relativistic dark matter is unlikely to make up most of the DM [5]. These evidences suggest the existence of a cosmologically significant abundance of nonbaryonic weakly interacting massive particles (WIMPs). Since SUSY models (including string inspired ones) generically predict new stable weakly interacting particles, the existence of WIMPs is even more likely.

Despite the fact that the nature of the DM is still unknown, it is usually thought that DM particles cannot be too heavy. If the WIMP is a thermal relic, then it was once in local thermodynamic equilibrium (LTE) in the early universe, and its present abundance is determined by its self-annihilation cross section. As argued by Griest and Kamionkowski [6], the self annihilation cross section has an upper bound of $\sim 1/M_X^2$ from considerations of unitarity, while the temperature at which freeze out occurs increases as the cross section is decreased. Hence, the assumption of LTE gives an upper bound of about 500 TeV to the mass of the dark matter. The present abundance of non-thermal relics (those that never attained LTE) is not determined by their self-annihilation cross section because their final abundance is not simply determined by the usual freeze out scenario. An example of a non-thermal relic is the axion, and the present axion abundance is determined by the dynamics of the phase transition associated with symmetry breaking. Non-thermal relics are typically very light, e.g., the axion mass is expected to be in the range 10^{-5} to 10^{-2} eV [7].

However, nonthermal relics can have masses many orders of magnitude larger than the electroweak scale and can evade the unitarity bound of Ref. [6]. These nonthermal DM particles have been called superheavy dark matter (SDM) in Ref. [8]. SDM scenarios have been discussed in conjunction with various production mechanisms (see for example [9] and references therein), with the gravitational production mechanism being arguably the least fine tuned [8, 10, 11]. In this paper, we will explore the idea of [12], which is to produce SDM by the same mechanism that is at work in what has been called “preheating” scenarios.

The main ingredient of the preheating scenarios, introduced in the early 1990s, is the nonperturbative resonant transfer of energy to particles induced by the coherently oscillating inflaton fields. It was realized that this nonperturbative mechanism can be much more efficient than the usual perturbative mechanism for certain parameter ranges of the theory [13, 14, 15, 16]. The basic picture can be seen as follows. Suppose we have a scalar field X with a coupling $g^2\phi^2X^2$ where ϕ is a homogeneous classical inflaton field. The mode equation for X field then can be written in terms of a redefined variable $\chi_k \equiv X_k a^{3/2}$ as

$$\ddot{\chi}_k(t) + (A + 2q \cos(2t))\chi_k(t) = 0 \tag{1}$$

where A depends on the energy of the particle and q depends on the inflaton field oscillation amplitude. When A and q are constants, this equation is usually referred to as the Mathieu equation which exhibits resonant mode instability for certain values of A and q . In an expanding universe, A and q will vary in time, but if they vary slowly compared to the frequency of oscillations, the effects of resonance will remain. If the mode occupation number for the X particles is large, the number density per mode of the X particles will be proportional to $|\chi_k|^2$. If A and q have the appropriate values for resonance, χ_k will grow exponentially in time, and hence the number density will

attain an exponential enhancement above the usual perturbative decay. This period of enhanced rate of energy transfer has been called preheating primarily because the particles that are produced during this period have yet to achieve thermal equilibrium.

This resonant amplification leads to an efficient transfer of energy from inflatons to other particles which may have stronger coupling to other particles than the inflaton, thereby speeding up the reheating process and leading to a higher reheating temperature than in the usual scenario. Another interesting feature is that particles of mass larger than the inflaton mass can be produced through this coherent resonant effect. Such a process is negligible in a conventional scenario of reheating [17]. This has been exploited to construct a baryogenesis scenario [12] in which the baryon number violating bosons with masses larger than the inflaton mass are created through the resonance mechanism. A natural variation on this idea is to produce SDM by the same resonance mechanism [12].

Interestingly enough, what we find in our work is that in the context of a slow-roll inflation with the potential $V(\phi) = m_\phi^2 \phi^2/2$ with the inflaton coupling of $g^2 \phi^2 X^2/2$, the resonance phenomenon is mostly irrelevant to the production of SDM because too many particles are produced when the resonance is effective. For the tiny amount of energy conversion needed for SDM production (tiny means $\sim 10^{-17}$ of the total energy), the coupling g^2 must be small enough (for a fixed M_X) such that the motion of the inflaton field only at the transition out of the inflationary phase generates just enough nonadiabaticity in the mode frequency to produce SDM. The rest of the oscillations, damped by the expansion of the universe, will not contribute significantly to particle production as in the resonant case. In other words, the quasi-periodicity necessary for a true resonance phenomenon is hardly existent for the case when only an extremely tiny fraction of the energy density is converted into SDM. Of course, if the energy scales are lowered such that a fair fraction of the energy density can be converted to DM without

overclosing the universe, this argument may not apply. However, in this paper, we will be mostly interested in producing SDM with masses larger than the inflaton mass within the context of a large-field inflationary scenario, where this argument will apply. For the study of cases in which the resonance starts to become efficient, we refer the reader to Refs. [18, 15, 13, 12] and references therein.

The main findings of this work are the following: We find that superheavy dark matter with a mass as large as $10^3 H_i$, where H_i is the value of the Hubble expansion rate at the end of inflation, can be produced in sufficient abundance to be cosmologically significant today. Typically, H_i can be as large as 10^{13} GeV, which means that the dark matter may have masses of the order of the GUT scale. In the process of finding this estimate, we derive a simple formula (in the spirit of Ref. [19]), Eq. (41), that can be used to estimate particle production resulting from a general class of interactions with a time varying homogeneous classical field (including the gravitational field). Finally we observe that coupling X to the inflaton field can actually decrease the amount of SDM produced as a consequence of the inflaton field variation canceling some of the nonadiabaticity of the expansion rate responsible for gravitational production of SDM.

This paper is organized as follows. In the next section we will specify the model and the inflationary scenario in which our estimations are carried out. In section III, we derive a general formula to estimate particle production when a quantum field interacts weakly with a general class of homogeneous classical fields. We then compare our approximations to two exact solutions. Section IV follows where we apply the estimation to our model described in Section II. We then present numerical results for comparison and a better estimation of the maximum cosmologically interesting SDM mass in our model. Finally, we conclude with a summary in Section V.

II. MODEL

Two conditions are necessary for the viability of the SDM scenario [8]: *a)* their interaction rate must be sufficiently weak such that local thermodynamic equilibrium (LTE) was never obtained and *b)* the X particles must be cosmologically stable. As we will see, because LTE necessitates the reaction rate to be larger than the Hubble expansion rate while the reaction rate involves at least an inverse mass squared suppression coming from the cross section involved, large mass particles can naturally evade LTE.

Let us denote ρ_X as the energy density of the SDM particles and $n_X(t_e)$ as the number density of the SDM at time t_e when inflation ends. As shown in [8], today's SDM density $\Omega_X \equiv \rho_X(t_0)/\rho_C(t_0)$ (where $\rho_C(t_0) = 3H_0^2 M_{\text{Pl}}^2/8\pi$ and $H_0 = 100 h \text{ km sec}^{-1} \text{ Mpc}^{-1}$) can be expressed as

$$\Omega_X h^2 \approx \Omega_R h^2 \left(\frac{T_{\text{RH}}}{T_0} \right) \frac{8\pi}{3} \left(\frac{M_X}{M_{\text{Pl}}} \right) \frac{n_X(t_e)}{M_{\text{Pl}} H_i^2} \quad (2)$$

where H_i is the Hubble expansion rate at the end of inflation, T_0 is the temperature today, T_{RH} is the reheating temperature, and $\Omega_R h^2 \approx 4.31 \times 10^{-5}$ is the fraction of critical energy density that is in radiation today. Throughout this paper, we will give our results in terms of $\Omega_X h^2/S$ where we have defined

$$S \equiv (T_{\text{RH}}/(10^9 \text{ GeV}))(H_i/(10^{-6} M_{\text{Pl}}))^2. \quad (3)$$

For a typical reheating temperature of 10^9 GeV, Eq. (2) implies that the SDM energy density today will be $\Omega_X h^2 \sim 10^{17}(\rho_X(t_e)/\rho(t_e))$ where $\rho(t_e)$ is the total energy density at the end of inflation. It is indeed a very small fraction of the total energy density that needs to be extracted to saturate the upper bound on the cosmological mass density. Hence, the difficulty of our scenario lies in creating very few particles, if these are to be the SDM.

Now, consider the nonthermalization condition

$$n_X \langle \sigma_A | v | \rangle \lesssim H \tag{4}$$

which allows the evasion of the unitarity upper bound on the mass of DM. Using Eq. (2) with $\Omega_X h^2 < 1$ and the fact that for WIMPS, the averaged annihilation cross section $\langle \sigma_A | v | \rangle$ is less than M_X^{-2} (unitarity bound), we can obtain the estimate

$$\frac{n_X \langle \sigma_A | v | \rangle}{H_i} < \frac{7 \times 10^{-19}}{(T_{\text{RH}}/10^9 \text{GeV})} \frac{(H_i/M_{\text{Pl}})}{(M_X/M_{\text{Pl}})^3} \tag{5}$$

which is the quantity that must be less than one at the end of inflation to avoid thermalization. If $H_i \approx 10^{-6} M_{\text{Pl}}$ and

$$\left(\frac{M_X}{H_i} \right) \left(\frac{T_{\text{RH}}}{10^9 \text{GeV}} \right)^{1/3} > 10^{-2}, \tag{6}$$

there is no LTE, and the particles density will evolve trivially as was assumed in Eq. (2). Thus, because of the M_X^{-2} generically coming from the cross section, SDM will generally fail to achieve LTE irrespective of the exact value of the weak coupling constant. Note that this is a rather conservative estimate since the reheating temperature is likely to be larger and the cross section is likely to be smaller. We also remark that because the reheating temperature is usually much smaller than the X mass in SDM scenarios, the thermal production of the X particles is usually negligible.¹

For the X particles to serve as DM, they must have a lifetime that is longer than the age of the universe and be extremely massive. One possible source of SDM is the secluded and the messenger sectors of the gauge mediated SUSY breaking models where SUSY can be broken at a large scale (giving rise to large masses) while the secluded and the messenger sectors can have accidental symmetries analogous to the baryon number

¹Since for times larger than t_e , the interaction rate continues to be smaller than H , the particles will not thermalize later either.

giving the particles stability [21, 22]. Other natural possibilities include theories with discrete gauge symmetries [24] and string/M theory [25].

To explore the dynamics which we believe is typical towards the end of inflation, we primarily focus on two coupled scalar fields in an expanding universe. The action can be written as

$$S = S_g + S_M \tag{7}$$

where

$$S_g = - \int d^4x \sqrt{-g} \frac{M_{\text{Pl}}^2 R}{16\pi} \tag{8}$$

$$S_M = \int d^4x \sqrt{-g} \left\{ \frac{1}{2} [g^{\mu\nu} \phi_{,\mu} \phi_{,\nu} - m_\phi^2 \phi^2] + \frac{1}{2} [g^{\mu\nu} X_{,\mu} X_{,\nu} - (m_X^2 + \xi R + g^2 \phi^2) X^2] \right\}. \tag{9}$$

We will take $\xi = 1/6$ corresponding to conformal coupling to gravity although our main results will be insensitive to this assumption. Neglecting the small effects coming from the quantum fluctuations, we take the gravitational field and the inflaton field to be purely classical fields. Note that we are neglecting other fields which the inflaton field needs to couple to in order to reheat the universe. We have numerically verified that as long as the reheating or preheating occurs on a time scale that is greater than $5m_\phi^{-1}$, our main conclusions are insensitive to this assumption since the particle production that is mainly of interest to us occurs during this time (as we will later see, nonresonant, nonperturbative production is of interest for superheavy dark matter production).

We will consider a metric of the form $ds^2 = dt^2 - a^2(t) d\mathbf{x}^2$. The resulting equations of motion for the homogeneous classical fields are

$$\frac{\dot{a}^2}{a^2} - \frac{4\pi}{3} (\dot{\phi}^2 + m_\phi^2 \phi^2) = 0 \tag{10}$$

$$\ddot{\phi} + 3 \frac{\dot{a}}{a} \dot{\phi} + m_\phi^2 \phi = 0 \tag{11}$$

where we have neglected the dark matter contribution to the energy density. This is a good approximation during the time period of dynamical interest.

Of course, we do not expect any of our results to be sensitive to the initial conditions, since our results depend upon what happens towards the end of inflation and afterwards. Our results will mainly depend upon the functional form of the potential for the inflaton field. In this paper, we will not study this model dependence but will study what we consider to be the typical dynamics of such systems. For the sake of completeness, we discuss in the Appendix the initial conditions that we use for our study.

Now let us consider the X sector. With the canonical conjugate to X as $a^3\dot{X}$ and canonically quantizing this action, the Heisenberg equation of motion is

$$\ddot{X} + 3H\dot{X} - \frac{1}{a^2}\nabla^2 X + (M_X^2 + g^2\phi^2)X = 0 \quad (12)$$

where $H = \dot{a}/a$ is the Hubble expansion rate. We introduce the Fourier convention

$$X = \int \frac{d^3k}{(2\pi)^{3/2}a} (a_k e^{i\vec{k}\cdot\vec{x}} h_k(t) + a_k^\dagger e^{-i\vec{k}\cdot\vec{x}} h_k^*(t)) \quad (13)$$

where we have defined $h_k = X_k a$ and defined the normalization for the annihilation operator as $[a_{\vec{k}_1}, a_{\vec{k}_2}^\dagger] = \delta^{(3)}(\vec{k}_1 - \vec{k}_2)$. Imposing the canonical commutation condition, we obtain the normalization condition

$$h_k \dot{h}_k^* - h_k^* \dot{h}_k = \frac{i}{a}. \quad (14)$$

The mode equation satisfied by h_k is

$$\ddot{h}_k + H\dot{h}_k + \left[-H^2 - \frac{\ddot{a}}{a} + \left(\frac{k}{a}\right)^2 + (M_X^2 + g^2\phi^2) \right] h_k = 0. \quad (15)$$

In conformal coordinates defined by $ds^2 = a^2(\eta)(d\eta^2 - d\mathbf{x}^2)$, this mode equation becomes

$$h_k''(\eta) + \omega_k^2 h_k = 0 \quad (16)$$

where $\omega_k = \sqrt{k^2 + (M_X^2 + g^2\phi^2(\eta))a^2(\eta)}$ and the $'$ derivative is with respect to conformal time.

Now we need to fix the boundary conditions. Because the particle number can be constant only for time translationally invariant systems, the no-particle state (the vacuum state) existing towards the end of inflation can be specified only approximately in an expanding universe (see, for example, [27] and [28]). One method of systematically classifying the various inequivalent approximate vacuum states is through the adiabatic vacuum [27] definition. As will be seen later, we will use an effectively infinite adiabatic order vacuum boundary conditions by considering the boundary conditions placed at arbitrarily far past and future for the nonsingular spacetime that we will consider.

If we denote $h_k^{\eta_1}$ as the mode solution with boundary conditions defined at a future time η_1 and $h_k^{\eta_0}$ as the mode solution with the boundary conditions defined at a time in the past η_0 , we can define the Bogoliubov transformation as $h_k^{\eta_1}(\eta) = \alpha_k h_k^{\eta_0}(\eta) + \beta_k h_k^{*\eta_0}(\eta)$. The number density then is given by

$$n_X(t) = \int_0^\infty \frac{dk}{2\pi^2 a^3(t)} k^2 |\beta_k|^2. \quad (17)$$

III. STEEPEST DESCENT METHOD

This section presents a derivation of the analytic estimation (Eq. (41)) that will be used in conjunction with the numerical work. A reader interested only in its application should skip to the next section. Its direct application to our physical system of main interest (presented in Section II) will be given in Section IV. The following analysis is in the spirit of Ref. [19].

With the definition

$$h_k = \frac{\alpha_k}{\sqrt{2\omega_k}} e^{-i \int \omega_k d\eta} + \frac{\beta_k}{\sqrt{2\omega_k}} e^{i \int \omega_k d\eta} \quad (18)$$

the differential equation

$$h_k'' + \omega_k^2 h_k = 0 \quad (19)$$

is equivalent to

$$\begin{aligned} \alpha_k' &= \frac{\omega_k'}{2\omega_k} \exp\left(2i \int \omega_k d\eta\right) \beta_k \\ \beta_k' &= \frac{\omega_k'}{2\omega_k} \exp\left(-2i \int \omega_k d\eta\right) \alpha_k. \end{aligned} \quad (20)$$

Because $\omega_k'/(2\omega_k)$ vanishes at $\eta = \pm\infty$ (adiabatic in-out region assumption), α_k and β_k become constants there, assuming no singular behavior occurs there. Expanding α_k and β_k in an adiabatic series (in powers of derivatives), and using the boundary condition $\alpha_k(\eta_p) = 1$ and $\beta_k(\eta_p) = 0$ (equivalent to an infinite adiabatic order boundary condition in the limit $\eta_p \rightarrow -\infty$ for our restricted class of spacetime) we obtain

$$\beta_k \approx \int d\eta \frac{\omega_k'}{2\omega_k} \exp\left(-2i \int^\eta \omega_k(\eta') d\eta'\right). \quad (21)$$

to leading order. Note that this approximation should be good as long as $\beta_k \omega_k'/(2\omega_k) \ll 1$ even when $\omega_k'/(2\omega_k) > 1$. This is certainly true for the cases to which we wish to apply this analysis. Our next objective is to obtain an approximation for this integral. Let us write

$$\omega_k = \sqrt{k^2 + M_X^2 C(\eta)} \quad (22)$$

where all the η dependence is contained in $C(\eta)$ and the radicand is positive definite for all real η . For example, in our model,

$$C(\eta) = \left(1 + \frac{g^2 \phi^2(\eta)}{M_X^2}\right) a^2(\eta) \quad (23)$$

which can be thought of as the square of an “effective” scale factor. We will also assume that $C(\eta)$ is C^∞ for real η and analytically continue ω_k to the complex plane. Because of the squareroot in the exponent, the poles of the integrand in Eq. (21) will also be

branch points in the complex η plane.² We will choose the branch cuts such that they go from the branch points to infinity along a path such that the branch points on the lower half plane have the cut going towards $-i\infty$ and the branch points on the upper half plane have the cut going towards $i\infty$. Furthermore, the cut will be taken along the curve where the exponential function has an equal modulus. Transverse to the cut, the exponential will fall off rapidly.

The integral over the real axis can be replaced (using Cauchy's theorem) with the integral over an appropriately deformed contour in the lower or upper half plane (we will soon see that our phase convention is such that we are really concerned with the poles on the lower half plane as shown in Fig. 1). The main contribution from the integral over the deformed contour will come from near the branch points and possibly the end points. The branch points will be distributed symmetrically with respect to reflection across the real axes because of the Schwartz reflection principle. The end point contribution will be of the order of ω'_k/ω_k . However, in our restricted class of spacetimes which admits an infinite adiabatic order vacua, we can make this contribution arbitrarily small by taking the endpoints further out. (We comment further on this effect later.) Hence in general, Eq. (21) can be approximated as a coherent sum of steepest descent integrals around each of the branch points.

Let us look at the contribution from the j th branch point denoted as $\tilde{\eta}_j$. Near this branch point, the integral in the exponent of Eq. (21) can be expanded as

$$\int_{\eta_p}^{\eta} \omega_k(\eta) d\eta = \int_{\eta_p}^{\tilde{\eta}_j} \omega_k(\eta) d\eta + \frac{2M_X}{3} \sqrt{C'(\tilde{\eta}_j)} \delta^{3/2} + \dots \quad (24)$$

where $\delta \equiv \eta - \tilde{\eta}_j$ and we kept the leading term in the δ expansion of C (we will assume that C' does not vanish here). Expanding in a similar way ω'_k/ω_k in Eq. (21), we can

²We assume that the integral of the squareroot in the exponent will introduce no other branch points.

write the contribution to β_k from this branch point as

$$U_j \equiv v_j \exp(-2i \int_{\eta_p}^{\tilde{\eta}_j} \omega_k(\eta) d\eta) \quad (25)$$

where we defined v_j as

$$v_j \equiv \frac{1}{4} \int_{C_j} \frac{d\delta}{\delta} \exp\left(\frac{-4i}{3} M_X \sqrt{C'(\tilde{\eta})} \delta^{3/2}\right) \quad (26)$$

and U_j was introduced to rewrite β_k as

$$\beta_k \approx \sum_j U_j. \quad (27)$$

Here the contour C_j near $\tilde{\eta}_j$ is the steepest descent contour.

Let us determine the steepest descent path near $\tilde{\eta}$. If we denote $\theta_2 \equiv \arg(C'(\tilde{\eta}))$ and denote θ to be the argument of δ along the steepest descent contour, the restriction on θ is

$$\theta = \frac{\pi(4n - 1) - \theta_2}{3} \quad (28)$$

where n is an integer. Now, if we let the branch cut go along $\arg(\delta) = \alpha$ such that $\arg(\delta) \in [\alpha, \alpha + 2\pi)$ on the lower half plane and $\arg(\delta) \in (\alpha - 2\pi, \alpha]$ on the upper half plane, upon choosing $\sqrt{C'(\eta)} > 0$ when η is real (consistent with positive frequency mode definition), we can place the restriction $\theta_2 \in [-\alpha, 2\pi - \alpha)$ in the upper half plane and $\theta_2 \in (-2\pi - \alpha, -\alpha]$ in the lower half plane. As mentioned above, we choose the branch cuts to go towards $\pm i\infty$ by restricting $\alpha \in (0, \pi)$ on the upper half plane and $\alpha \in (-\pi, 0)$ on the lower half plane. Finally, restricting the branch cut to be on an equal modulus curve, we obtain the relationship

$$\alpha = \frac{-\theta_2 \pm 2\pi}{3} \quad (29)$$

where the positive sign corresponds to the upper half plane and the negative sign corresponds to the lower half plane.

Combining Eqs. (28) and (29), we find two possible integers $n = 0, 1$ for the lower half plane, while we find only one possible integer $n = 0$ for the upper half plane. Since the steepest descent approximation requires an incoming direction and an outgoing direction for each of our branch points, we can only use the lower half plane branch points. To summarize, the necessity of making branch cuts with the appropriate shape and the information regarding the derivative of C at the branch point determines the usable steepest descent paths, which are restricted to the lower half plane (lower and not upper because of the sign convention on the squareroot). This, as we will see below, corresponds to an exponentially damped result.

Let us return to the evaluation of v_j in Eq. (26). From Eq. (28) and Eq. (29), we see that the branch cut bisects the angle made by the steepest descent contour which makes a fixed (acute) angle of $2\pi/3$ (or $4\pi/3$ in coordinate angle), and hence the steepest descent path is well defined independently of θ_2 . Hence, we can easily evaluate the integral after making a change of variables $u = \delta^{3/2}(-4im\sqrt{C'(\tilde{\eta}_j)}/3)$. The result is

$$v_j = \frac{i\pi}{3} \tag{30}$$

Now we need to evaluate

$$\int_{\eta_p}^{\tilde{\eta}_j} \omega_k(\eta) d\eta \tag{31}$$

to complete our evaluation of U_j . Since we do not in general know the function $C(\eta)$ on the complex plane but know it and its derivatives on the real axis (numerically for the model presented in section II), let us find an estimation utilizing that ω_k is analytic around the real axis. Let $\tilde{\eta}_j = r + \mu$ where r is purely real and μ is purely imaginary. Now, we split the integral into

$$\int_{\eta_p}^{\tilde{\eta}_j} \omega_k(\eta) d\eta = \Phi_j + J_j \tag{32}$$

where

$$\Phi_j = \int_{\eta_p}^r \omega_k(\eta) d\eta \quad (33)$$

$$J_j = \int_r^{\tilde{\eta}_j} \omega_k(\eta) d\eta \quad (34)$$

where Φ_j is purely real. To evaluate J_j , we expand in Taylor series,

$$J_j \approx \omega_k(r)\mu + \omega'_k(r)\mu^2/2 + \omega''_k(r)\mu^3/6 + \dots \quad (35)$$

where one should note that all the even terms are real. Because we will mainly be interested in one pole domination case, we will only calculate the imaginary value of J_j .

Thus, as long as

$$|\omega''_k/\omega_k| \ll |6/\mu^2| \quad (36)$$

we can truncate the J_j after the first term. We shall check the self consistency later.

To approximate $\tilde{\eta}_j$, we Taylor expand the left hand side of $C = -(k/M_X)^2$ about r to obtain

$$\frac{\mu^2}{6} C'''(r) + C'(r) = 0 \quad (37)$$

$$\frac{\mu^2}{2} C''(r) = -\frac{\omega_k^2(r)}{M_X^2} \quad (38)$$

where $C'''(r) > 0$ since μ is purely imaginary. The truncation of the Taylor expansion should be justified as long as

$$\left| \frac{C^{(5)}(r)}{C'''(r)} \right| \frac{\omega_k^2}{10M_X^2 C''(r)} \ll 1 \quad (39)$$

$$\frac{|C^{(4)}(r)|}{C''(r)^2} \frac{\omega_k^2}{6M_X^2} \ll 1 \quad (40)$$

for Eqs. (37) and (38) respectively where the superscript indicates the order of the derivative.³

³Note that even if Eq. (39) is not satisfied, all the equations derived may still be valid as long as r can be estimated another way.

Assuming that the contribution from one of the poles dominates in Eq. (27), we can approximate $|\beta_k|^2 \approx |U_1|^2$. Using Eq. (38) and choosing the solution on the lower half plane (as we have justified above), we obtain

$$|\beta_k|^2 \approx \exp \left(-4 \left[\frac{(k/a_{\text{eff}}(r))^2}{M_X \sqrt{H_{\text{eff}}^2(r) + R_{\text{eff}}(r)/6}} + \frac{M_X}{\sqrt{H_{\text{eff}}^2(r) + R_{\text{eff}}(r)/6}} \right] \right) \quad (41)$$

where we have dropped the factor of $(\pi/3)^2$, we have defined the effective scale factor

$$a_{\text{eff}} = \sqrt{C}, \quad (42)$$

and $H_{\text{eff}}(r)$ and $R_{\text{eff}}(r)$ correspond to Hubble expansion rate and Ricci scalar (respectively) for the metric $ds^2 = a_{\text{eff}}^2(\eta)(d\eta^2 - d\mathbf{x}^2)$. All time dependent quantities in Eq. (41) are evaluated at $\eta = r$ given by Eq. (37). Explicitly, the radicand of the exponent in Eq. (41) is simply $H_{\text{eff}}^2(r) + R_{\text{eff}}(r)/6 = C''(r)/(2C^2(r))$ since $6a_{\text{eff}}''/a_{\text{eff}}^3 = R_{\text{eff}}(r)$ and $a_{\text{eff}}'/a_{\text{eff}}^2 = H_{\text{eff}}(r)$. Rewriting the condition Eq. (36) in this new notation as (in the $k \rightarrow 0$ limit)

$$6H_{\text{eff}}^2(r) + R_{\text{eff}}(r) \gg R_{\text{eff}}(r)/6 \quad (43)$$

we see that this condition is almost always satisfied as long as the Eq. (40) is satisfied.⁴

The exponentially suppressed behavior is not exact for arbitrarily large masses since the endpoint contribution will eventually become larger. An asymptotic analysis of the problem in the appendix of [8] gives the general power law mass dependence of the endpoint contribution. As discussed there, this contribution can become particularly significant when C is not analytic. The present analysis, however, shows that owing to the fact the endpoints lie far away from the branch points (which have stationary phases), in the case that C is analytic, the contribution from the endpoints can be made arbitrarily small as long as the spacetime admits an infinite adiabatic order in-out regions.

⁴Eq. (40) must be satisfied since we are using Eq. (38) to get the value of μ .

Let us restate the main point of this somewhat technical section. Given a homogeneous classical field coupling that gives rise to mode equations of the form Eq. (19) with ω_k given by Eq. (22) and given an in-out infinite adiabatic order vacua, the Bogoliubov coefficient giving the particle density per mode is given by Eq. (41) and the number density is given by⁵

$$n_X(t) \approx \frac{a_{\text{eff}}^3(r)}{8\pi^{3/2}a^3(t)} \exp\left(\frac{-4M_X}{\sqrt{H_{\text{eff}}^2(r) + R_{\text{eff}}(r)/6}}\right) \left[\frac{M_X}{4}\sqrt{H_{\text{eff}}^2(r) + R_{\text{eff}}(r)/6}\right]^{3/2} \quad (44)$$

where $a_{\text{eff}}(r)$, $R_{\text{eff}}(r)$, and $H_{\text{eff}}(r)$ are effective scale factor, Ricci scalar, and Hubble expansion rate defined by Eq. (42) and the statement following it. The “effective” quantities are all evaluated at a value of r satisfying Eqs. (37) and (38). As will be discussed towards the end of next section, r is roughly the point at which C varies nonadiabatically, or a bit more precisely, where $C'''(r)/C^2(r)$ is a maximum. For couplings of the form $Q(\phi)X^2/2 + \xi RX^2/2$ where Q is analytic and R is the Ricci scalar of the spacetime, we can write

$$C(\eta) = a^2(\eta)(1 + Q(\phi)/M_X^2 + (\xi - 1/6)R/M_X^2) \quad (45)$$

in a spacetime with the metric $ds^2 = a^2(\eta)(d\eta^2 - d\mathbf{x}^2)$.

IV. COMPARISON WITH EXACT RESULTS

Let us first apply Eq. (41) to a couple of exactly soluble cases. Consider the case given by Ref. [30] when there is no inflaton coupling to the X field and the spacetime is

⁵ Although r in general depends on k (for an explicit example, see Eq. (58)), because most of the contribution to the number density comes from $(k/M_X)^2 \ll 1$ where the k dependence can be neglected, we shall neglect k when doing the momentum integral.

given by $ds^2 = C(\eta)(d\eta^2 - d\mathbf{x}^2)$ where

$$C(\eta) = c_1^2 + c_2^2\eta^2 \quad (46)$$

where c_1 and c_2 are real constants. The exact number density per mode is

$$|\beta_k|^2 = \exp\left(-\pi\left[\frac{k^2}{M_X c_2} + \frac{M_X c_1^2}{c_2}\right]\right) \quad (47)$$

which has been noted [30] as the spectrum of a nonrelativistic gas of particles with momentum k/\sqrt{C} having chemical potential of $-M_X c_1^2/(2C)$ and a temperature of $c_2/(2\pi C)$

In deriving Eq. (41), we have made two separate approximations. One is the usage of the steepest descent method and the other is the estimation of the integral Eq. (31). To test the goodness of each of these approximations, since we know C exactly here, we will first consider the steepest descent method with the exact branch point. Let's start from Eqs. (25) and (27). One branch point is on the lower half plane at

$$\eta = \tilde{\eta} \equiv -i\sqrt{\frac{c_1^2 + k^2/M_X^2}{c_2^2}} \quad (48)$$

and another, its complex conjugate, is on the upper half plane. The quantity v_j has been already evaluated in general, corresponding to a contour integral around the branch point on the lower half plane, and is given by Eq. (30). The integral Eq. (31) can be easily calculated with $\tilde{\eta}_j = \tilde{\eta}$ to give

$$\int_{\eta_p}^{\tilde{\eta}_j} \omega_k(\eta) d\eta = (-i\pi/2 + \text{real phase}). \quad (49)$$

Putting this in Eq. (25), we have

$$|\beta_k|^2 \approx \left(\frac{\pi}{3}\right)^2 \exp\left(-\pi\left[\frac{k^2}{M_X c_2} + \frac{M_X c_1^2}{c_2}\right]\right) \quad (50)$$

whose exponent we see matches the exact result of Eq. (47).

Now, let's apply Eq. (41). Eq. (37) gives $r = 0$. Hence, we find

$$|\beta_k|^2 \approx \exp\left(-4\left[\frac{k^2}{M_X c_2} + \frac{M_X c_1^2}{c_2}\right]\right) \quad (51)$$

which gives only an approximately correct exponent. However, note that the functional form of the mass dependence of the exponent is exact. Hence, although the steepest descent approximation seems to give accurate results for the exponent, as exemplified by Eq. (50), the Taylor expansion method used to estimate the integral Eq. (31) leads to a numerical value of the exponent that is only roughly correct as seen in Eq. (51). Still we see the functional behavior of the mass dependence is accurate.

Let's consider another exactly soluble case [31] (see also [28]) specified by

$$C(\eta) = A + B \tanh(\rho\eta) \quad (52)$$

where A , B , and ρ are positive constants with $A > B$. This results in particle density per mode of

$$|\beta_k|^2 = \frac{\sinh^2 \left\{ \frac{\pi}{2\rho} \left[\sqrt{k^2 + M_X^2(A+B)} - \sqrt{k^2 + M_X^2(A-B)} \right] \right\}}{\sinh \left[\frac{\pi}{\rho} \sqrt{k^2 + M_X^2(A-B)} \right] \sinh \left[\frac{\pi}{\rho} \sqrt{k^2 + M_X^2(A+B)} \right]}. \quad (53)$$

When the exponential cut off starts to become effective for large masses, the behavior is

$$|\beta_k|^2 \approx \exp \left(-\frac{2\pi M_X}{\rho} \sqrt{A-B} \right) \quad (54)$$

where we have effectively set $k = 0$. Let us compare this with the steepest descent approximation. In this example, it is easier to find the branch point exactly. However, since we are interested in using the Taylor expansion estimation, let us solve Eqs. (37) and (38) which are valid if the conditions Eqs. (39) and (40) can be satisfied. These conditions are respectively

$$\left| \frac{4\rho^2(2 - 17t_r^2 + 30t_r^4 - 15t_r^6)}{(1 - t_r^2)(1 - 3t_r^2)} \right| \ll \frac{-20B\rho^2(1 - t_r^2)t_r}{(k/M_X)^2 + A + Bt_r} \quad (55)$$

$$\left| \frac{4\rho^2 t_r(2 - 5t_r^2 + 3t_r^4)}{(1 - t_r^2)t_r} \right| \ll \frac{-12B\rho^2(1 - t_r^2)t_r}{(k/M_X)^2 + A + Bt_r} \quad (56)$$

where we have defined $t_r \equiv \tanh(\rho r)$. Here, we know that $t_r < 0$ because

$$C'''(r) = -2B\rho^2(1 - t_r^2)t_r \quad (57)$$

must be positive as we explained before. Hence, we only need to consider $t_r \in (-1, 0]$ and find that our conditions imply $A \approx B$. Solving Eqs. (37) and (38) for t_r , we find

$$t_r = \frac{-B - \sqrt{B^2 + 3(A + (k/M_X)^2)^2}}{3(A + (k/M_X)^2)} \quad (58)$$

which then implies

$$\frac{C''(r)}{2C^2(r)} = \frac{4\rho^2}{9(A - B)} - \frac{\rho^2}{2B} + \mathcal{O}(A - B) \quad (59)$$

where we have expanded in powers of $A - B$ and set $k = 0$. Therefore, in the large mass limit, using again Eq. (41), we have

$$|\beta_k|^2 \approx \exp\left(-\frac{6M_X}{\rho}\sqrt{A - B}\right) \quad (60)$$

which is in reasonable agreement with Eq. (54). The lesson that we have learned here is that as long as one accounts for the regime in which the approximations are valid, the parameter dependence of the damping exponent is accurately calculated by our method.

Finally, we note that an intuitive meaning can be attached to the value of r . The quantity $H_{\text{eff}}^2(\eta) + R_{\text{eff}}(\eta)/6$ has a maximum at an $\eta = \eta_*$ satisfying the equation

$$C'C''' + CC'''' = 3C'C'' \quad (61)$$

which⁶ is very similar to the equation determining r

$$(k/M_X)^2 C'''' + CC'''' = 3C'C'' \quad (62)$$

Since $(k/M_X)^2 C'''' \sim C'C''$ (as can be seen by looking at Eqs. (61) and (41)) for important values of k and since η_* is a stationary point, we expect r to be very close to η_* . Therefore, r in general will roughly correspond to the most “nonadiabatic” point, i.e. the point at which $H_{\text{eff}}^2(\eta) + R_{\text{eff}}(\eta)/6$ is a maximum.

⁶Taking into account the validity condition for the Taylor expansion, it is easy to see that η_* indeed corresponds to a maximum.

For example, let us consider the model specified by Eq. (52). If one takes the branch point determining equation to be Eq. (61), then the resulting value of the number density per mode is

$$|\beta_k|^2 \approx \exp\left(-\frac{4\sqrt{2}M_X}{\rho}\sqrt{A-B}\right) \quad (63)$$

which is in reasonable agreement with Eqs. (60) and (54).

V. ANALYTIC ESTIMATION

Let us first consider the work of Ref. [18] to see what part of the parameter space we are interested in. Ref. [18] estimated the particle production in our type of system by neglecting any contribution from the decaying mode and using the Mathieu instability band plot to estimate the “average” exponent of the mode growth. (Recall that in an expanding universe, the mode equation is not exactly the Mathieu equation, since the parameters of what would be the Mathieu equation is time dependent in an expanding universe.) This method gives a good idea of when the particle production will be efficient through the resonance phenomenon.

Let’s start with the number density per mode written as

$$|\beta_k|^2 = \frac{\Omega_k}{2} \left(|\chi_k|^2 + \frac{1}{\Omega_k^2} |\dot{\chi}_k - \frac{\dot{a}}{2a} \chi_k|^2 \right) - 1/2 \quad (64)$$

where χ_k is the solution to the conformally coupled mode equation (15) with $\chi_k = \sqrt{a}h_k$ satisfying the 0th order adiabatic vacuum boundary condition in the past and $\Omega_k = \sqrt{(k/a)^2 + M_X^2 + g^2\phi^2}$. Approximate the relevant solution as

$$\chi_k \sim \frac{\exp(\int \mu m_\phi dt - i \int w_k dt)}{\sqrt{2w_k}} \quad (65)$$

where $w_k = \sqrt{\Omega_k^2 + (1/4)H^2 - (1/2)\dot{H}}$ and μ is the Mathieu characteristic exponent when the mode equation is written in the form of Eq. (1) (see below). The form of the

approximation is roughly equal to the lowest order adiabatic approximation and taking only the growing mode is justified by the fact that the decaying solution will be small in comparison. Now, approximating $w_k \approx \Omega_k$ and assuming $(\mu m_\phi)^2/(2\Omega_k^2) \ll 1$, we obtain the approximation

$$|\beta_k|^2 \sim \frac{1}{2}[\exp(2 \int \mu m_\phi dt) - 1] \quad (66)$$

which is the starting point in [18].⁷

The mode equation (15) with $\chi_k = \sqrt{a}h_k$, when written in the form of the Mathieu equation Eq. (1) gives

$$\begin{aligned} A &\approx \left(\frac{k}{am_\phi}\right)^2 + \left(\frac{M_X}{m_\phi}\right)^2 + 2q + 2/(3m_\phi t)^2 \\ q &\approx \frac{g^2\Phi(t_0)^2}{4m_\phi^2(m_\phi t)^2} \end{aligned} \quad (67)$$

where we have chosen the initial time to be at $t = t_0 = 1/m_\phi$ and $\Phi(t_0)$ represents the amplitude of the inflaton field oscillations at the initial time when the inflaton field oscillation amplitude starts to decay like $1/t$ in a pressureless universe. Ref. [18] then considers the trajectory of these parameters as a function of time and estimates the exponent integral in Eq. (66). They find that the efficient preheating ceases at around $M_X = 100m_\phi$ for $g < 1$. After that, the incoherent decay process dominates the energy release of the inflaton.

In our case, we are more interested in the regime in which the resonance phenomenon is extremely ineffective, or virtually non-existent, because only an extremely tiny density of very massive particles is allowed for the dark matter scenario. Define the parameter $b = M_X/H_i$ where H_i is the value of the Hubble parameter at the end of inflation. Consider the case when $b = 7$ and $g = 0$, for which $\Omega_X h^2/S = 0.128$. When the

⁷They had used minimal coupling to gravity, but as we can see that is of little importance as far as the approximation Eq. (66) is concerned.

interaction is turned on to say $gM_{\text{Pl}}/H_i = 45$, we find that there is a factor of 100 increase in the particle density produced to $\Omega_X h^2/S = 12$. As illustrated in Fig. 2, we see that for this value of gM_{Pl}/H_i , b , and values of k that dominate the integral for the mode sum, the Mathieu parameter trajectories never cross any of the instability bands. Thus, the analysis of Ref. [18] is only partially applicable to our case, mostly because we are only requiring a very small fraction of the inflaton energy density to turn into X particles. This means that the X particle masses that can be produced in interesting quantities should be significantly greater than $100m_\phi$ for coupling constants still less than 1. Furthermore, since significant dark matter production occurred without the trajectories ever crossing any of the instability bands, we can expect sufficient dark matter to be generated without any resonance effects.

Now let us apply the estimation of Eq. (41) to the system presented in Section II. Let us consider the largest possible perturbative coupling of around $gM_{\text{Pl}}/H_i = 10^6$ which is what would give the largest possible mass for the dark matter produced.⁸ We first look for the solutions to Eqs. (37) and (38). There are many solutions to these equations, as we expect. However, only one of these solutions will be relevant for the one pole domination approximation. To see which solution will be relevant, we plot in Fig. 3 the absolute value of the exponent in Eq. (44) which we will denote as τ , as a function of time values that are near the actual solution to Eqs. (37) and (38). For definiteness, we will fix b at 1080 although the one pole domination approximation will be reasonable for all other masses within the range of our interest. It is clear from these plots that the pole having a real part corresponding to $t \approx 109$ will dominate in the sum Eq. (27), thereby justifying the one pole approximation reflected in Eq. (41). In Fig. 3, we have also plotted the case of $gM_{\text{Pl}}/H_i = 10^3$ and $b = 30$ to indicate the generic nature of this

⁸ We are assuming here that something like SUSY is protecting the inflaton potential from large radiative corrections that can spoil inflation.

one pole domination.

The solutions to Eq. (37) and Eq. (38) that is of interest to us are not sensitive to the value of $b \equiv M_X/H_i$ as long $gM_{\text{Pl}}/H_i/b \gg 1$ which turns out to be within our range of interest mainly because $\phi < M_{\text{Pl}}$ and $|\dot{\phi}/H_i| < M_{\text{Pl}}$ at the end of inflation as can be seen by looking at the exponent of Eq. (41). For example, with $k = 0$, the value of $t(r)$ that will be of interest to us is 108.90 (in units of $1/(12.2H_i)$) for both $b = 900$ and $b = 1800$. Only for values of b as large as 10^4 (which we will not be of much interest to us), does the value of $t(r)$ deviate to 108.89. The dependence on k , which can be seen directly in Eqs. (37) and (38) will also be negligible because the most of the SDM that are produced will be nonrelativistic.

Hence, with $t(r) = 108.9$ we use Eq. (41) to find that $\Omega_X h^2/S = 1$ at $b \approx 1450$ and $\Omega_X h^2/S = 0.01$ at $b \approx 1550$. Hence, taking $H_i \approx m_\phi/2$, the maximum possible mass of SDM for which its abundance will be cosmologically significant is an order of magnitude above the maximum mass that can accommodate efficient preheating. In the next section we will give a bit better estimate by taking into account the numerical calculation of the particle production.

Now, let us check the validity of truncating the Taylor expansion in approximating the location of the poles. The quantities on the left hand side of Eq. (40) and Eq. (39) are plotted in Fig. 4. From the figure it is clear that for the $gM_{\text{Pl}}/H_i = 10^6$ the approximation is well justified. However, the right hand panel of the figure shows that the approximation is only marginally adequate for $gM_{\text{Pl}}/H_i = 10^3$.

VI. NUMERICAL ESTIMATION

Because $|\beta_k|^2$ required to have $\Omega_X h^2/S \sim 1$ is extremely small and one must in general

compare oscillatory functions to obtain it, it is difficult to calculate it numerically. For $\Omega_X h^2/S \sim 1$, one requires an accurate calculation of

$$|\beta_{\bar{k}}|^2 \sim \frac{10^{-5}}{b^3(\bar{k}/(a_i H_i))^3} \quad (68)$$

where $\bar{k}/(a_i H_i)$, the average momentum component, is typically around $0.3b$. Hence, for $b \sim 10^6$, even with appropriate scaling, the calculation is numerically delicate. Furthermore, since many momentum components must be calculated for the integration of the spectrum to obtain the number density, an accurate calculation is time consuming, at least within a straight forward framework of calculation. The results presented in this section comes from a Runge-Kutta solution to a system of equations including Eqs. (15), (10), and (11), all appropriately scaled both in the independent and the dependent variables.

A sample of the numerical results are presented in Figs. 5 and 6. Motivated by our experience with the comparison with exactly soluble cases in section IV, where we have seen that the Taylor expansion approximation used gets the exponent correct only up to a constant multiplicative factor close to 1, we introduce a correction factor f in the exponent of Eq. (41) as

$$|\beta_k|^2 \approx \exp \left(-4f \left[\frac{(k/a_{\text{eff}}(r))^2}{M_X \sqrt{H_{\text{eff}}^2(r) + R_{\text{eff}}(r)/6}} + \frac{M_X}{\sqrt{H_{\text{eff}}^2(r) + R_{\text{eff}}(r)/6}} \right] \right) \quad (69)$$

and integrate this with respect to k to get $\Omega_X h^2/S$ that is plotted with the solid curve in Figs. 5 and 6. It is clear from the fact that f is about 1 in both the $gM_{\text{Pl}}/H_i = 10^6$ and $gM_{\text{Pl}}/H_i = 10^3$ cases that our analytic approximation is a reasonable one. Furthermore, as exemplified in Fig. 7, the fit to any particular spectrum by adjusting only f gives nearly an exact fit with f between 0.9 and 1.0. From Fig. 5, $M_X \sim 1700H_i \sim 10^3 m_\phi$ is the maximum possible value of superheavy dark matter that can be produced in cosmologically significant abundance in this inflationary scenario unless $H_i \gg 10^{-6} M_{\text{Pl}}$ or $T_{\text{rh}} \gg 10^9$ GeV.

Before concluding, we would like to note a phenomenon that occurs when the nonadiabaticity of the mode frequency change caused by the inflaton coupling is comparable to the nonadiabaticity caused by the gravitational coupling. If we crudely approximate the exponent of Eq. (41) as

$$-4 \left[\frac{(k/a_{\text{eff}}(r))^2}{M_X H_{\text{eff}}(r)} + \frac{M_X}{H_{\text{eff}}(r)} \right] \quad (70)$$

which is qualitatively reasonable in our scenario, then we can find using crude estimates made in the Appendix (i.e. $H_i \approx m_\phi/3$, $\phi \approx M_{\text{Pl}}/\sqrt{12\pi}$, and $\dot{\phi} \approx -M_{\text{Pl}}m_\phi/(2\sqrt{3\pi})$) that $\Omega_X h^2/S$ vanishes at $gM_{\text{Pl}}/H_i \approx 4b$. Of course, in reality the nonadiabaticity is not perfectly canceled, and we expect only a dip in the particle density as gM_{Pl}/H_i is increased from 0. Indeed, this cancellation of nonadiabaticity has been observed numerically as illustrated by Fig. 8. Hence, in general, for small positive g^2 couplings to the inflaton field, the particle production is not a monotonic function of the coupling constant because of the presence of the classical gravitational field.

VII. SUMMARY

In this article, we have considered the production of superheavy particles X that are coupled to a homogeneous classical inflaton field ϕ . We have found that within the context of a reasonable $V(\phi) = m_\phi^2 \phi^2/2$ slow-roll inflationary scenario with the coupling $g^2 X^2 \phi^2/2$, the parametric resonance phenomenon tends to overproduce the number of dark matter particles. Only when the resonance phenomenon completely shuts off is the number density small enough to be consistent with the constraint $\Omega_X h^2 < 1$. For the superheavy particles to be cosmologically significant today ($\Omega_X \sim 1$), its mass can be as large as about $1000H_i \sim 1000m_\phi$ as indicated by Fig. 5. Taking into account the COBE normalization of the curvature perturbation power spectrum, i.e. $2P_R^{1/2}/5 \approx 1.91 \times 10^{-5}$

at a scale of $k \approx 7.5H_0$ (see for example [32]), and using the approximation

$$\frac{2}{5}P_R^{1/2} = \frac{8^{3/2}\sqrt{\pi}}{\sqrt{75}M_{\text{Pl}}^3} \frac{V^{3/2}}{V'} \quad (71)$$

where the inflaton potential is evaluated at the time of horizon exit (about 50 e-folds before the end of inflation), we can estimate $m_\phi \sim 10^{13}$ GeV. This means that the mass of the dark matter particles can be of the order of the GUT scale.

In the process of making the superheavy dark matter mass range estimate, we have derived a simple general formula Eq. (41) giving an estimate of the particle production due to interactions with classical fields in the limit that there is only one, dominant nonadiabatic time period during which particle production “occurs.” The time dependent quantities in Eq. (41) can be approximately evaluated at the point at which $C'''(r)/C^2(r)$ (primes refer to conformal time derivatives) is a maximum, where for example, for couplings of the form $Q(\phi)X^2/2 + \xi RX^2/2$, C is given by Eq. (45). This result is applicable to almost any case of time varying homogeneous classical scalar field interacting with a quantum field as long as the number of particles produced is small.

Finally, we pointed out a phenomenon in which the number of X particles produced actually decreases as the coupling to the inflaton field ϕ increases (Fig. 8). This is a simple consequence of the fact that the nonadiabatic variation of the inflaton field is canceled out by the gravitational effect of nonadiabatic change in the scale factor.

As far as the observability of SDM is concerned, the prospects seem no better than in the case of electroweak scale WIMPs, unless the WIMPs are strongly interacting or charged. Previously, charged [33, 34] or strongly interacting dark matter [35] has been ruled out with a combination of arguments coming from the unitarity bound [6] and experimental observations. Since the SDM evades the usual unitarity bound, charged or strongly interacting dark matter may still be viable in this scenario.

If the SDM decays via an electromagnetic or a hadronic decay, its decay products

may change the spectrum of the diffuse gamma ray background [36]. Hence, the diffuse background photon measurements of EGRET and COMPTEL give strong constraints to such decaying particles for a fairly large range of life times. Note that Refs. [10, 37, 38] also suggest that if the SDM decays, its decay products may manifest in the form of ultrahigh energy cosmic rays. Note that in these decay scenarios, the life time must be in general much longer than the age of the universe. For example, according to Ref. [38], if the cosmic ray energy spectrum above 10^{11} GeV is produced by the decay of SDM, the lifetime of the SDM must be around $10^{12}\xi_X$ in units of the age of the universe where ξ_X is the fraction of the cold dark matter in SDM.

In general, we do not expect the direct WIMP detection experiments to be sensitive to SDM because of their low abundance. The detection rate which goes like $R \sim \rho_0 \sigma v / (M_X m_N)$ where ρ_0 is the matter density of the halo, σ is the elastic scattering cross section, v is the virial speed, and m_N is the mass of the nucleon. Hence, unless if the particles are strongly interacting in which case $\sigma \sim 10\text{mb}$ [39], the WIMP detectors will not have sufficient event rates to measure these particles.

The indirect method of dark matter detection (detecting the energetic neutrinos produced by annihilation of dark matter captured through elastic collisions [40]) will also have difficulty in the SDM scenario. The neutrino detection rate in general depends upon the SDM's capture rate in the sun through elastic collisions, its annihilation rate, and the neutrino cross section for the production of leptons in the rock or the detector. Since SDM mass will be much greater than that of the elastic scatterer, it will lose very little of its momentum per elastic collision (fractionally m_N/M_X where m_N is the mass of the nucleon). Hence, in addition to the small number density ($0.4 \text{ GeV}/\text{cm}^3/M_X$) to begin with, the capture probability through elastic collisions will be negligible. The annihilation rate will also be suppressed (unitarity bound $\sim 1/M_X^2$) even if one assumes maximal branching fraction to the neutrino producing channels. However, the the cross

section for the production of leptons in the rock or the detector will be significantly enhanced. Still, because the cross section will only grow like $\sqrt{M_X}$ for M_X much greater than the mass of W^\pm (assuming that the neutrinos will have energies that scale like M_X), the enhancement will not be sufficient to overcome the suppressions. Indeed, even if one neglects the neutrino absorption rate in the sun, if there is no significant accretion of SDM in the sun, one can easily show that the detection rate will be much smaller than the current detector sensitivity [40] of $10^{-2}\text{m}^{-2}\text{yr}^{-1}$.

Because the dark matter searches have focused mainly on those particles with masses that are less than about 100 TeV, the observational consequences for SDM have been relatively unexplored. Since as shown in Refs. [8, 9] and in this paper, production mechanisms exist for such particles, and since Refs. [21, 24, 25] has shown such particles exist in extensions to the standard model, a more careful study of observational consequences of SDM scenarios may be worthwhile.

ACKNOWLEDGMENTS

I thank Rocky Kolb for suggesting the problem and commenting insightfully regarding the manuscript. I also thank Michael Turner, Simon Swordy, and Emil Martinec for their comments on this work. This research was supported by the DOE and NASA under Grant NAG5-7092.

References

- [1] K. G. Begeman, A. H. Broeils and R. H. Sanders, *Mon. Not. R. Astro. Soc.* **249**, 523 (1991).

- [2] A. Dekel, *Ann. Rev. Aston. Astrophys.* **32**, 371 (1994).
- [3] K. A. Olive, G. Steigman, D.N. Schramm, T. P. Walker, and H. Kang, *Astrophys. J.* **376**, 51 (1991).
- [4] C. Copi, D. Schramm, and M. Turner, *Science* **267**, 192 (1995).
- [5] S. D. M. White, C. Frenk, and M. Davis, *Astrophys. J.* **274**, L1 (1983); J. Centrella and A. Melott, *Nature* **305**, 196 (1982).
- [6] K. Griest and M. Kamionkowski, *Phys. Rev. Lett.* **64**, 615 (1990).
- [7] G.G. Raffelt, Contribution to the Proceedings of *Beyond the Desert*, Ringberg Castle, Tegernsee, Germany June 8-14, 1997 (Preprint astro-ph/9707268).
- [8] D. J. H. Chung, E. W. Kolb, and A. Riotto, hep-ph/9802238.
- [9] D. J. H. Chung, E. W. Kolb, and A. Riotto, hep-ph/9805473.
- [10] V. Kuzmin and I. Tkachev, hep-ph/9802304.
- [11] T. Damour and A. Vilenkin, *Phys. Rev. D* **53**, 2981 (1996).
- [12] E. W. Kolb, A. D. Linde and A. Riotto, *Phys. Rev. Lett.* **77**, 4290 (1996); B. R. Greene, T. Prokopec and T. G. Roos, *Phys. Rev.* **D56**, 6484 (1997); E. W. Kolb, A. Riotto and I. I. Tkachev, hep-ph/9801306.
- [13] J. Traschen and R. Brandenberger, *Phys. Rev. D* **42**, 2491 (1990); Y.Shtanov, J. Traschen, and R. Brandenberger, *Phys. Rev. D* **51**, 5438 (1995).
- [14] L. A. Kofman, A. D. Linde and A. A. Starobinsky, *Phys. Rev. Lett.* **73**, 3195 (1994)
- [15] L. Kofman, A. D. Linde and A. A. Starobinsky, *Phys. Rev.* **D56**, 3258 (1997).

- [16] S. Yu. Khlebnikov and I. I. Tkachev, Phys. Rev. Lett. **77**, 219 (1996); Phys. Lett. **B390**, 80 (1997); Phys. Rev. Lett. **79**, 1607 (1997); Phys. Rev. **D56**, 653 (1997); G. W. Anderson, A. Linde and A. Riotto, Phys. Rev. Lett. **77**, 3716 (1996); see L. Kofman, *The origin of matter in the Universe: reheating after inflation*, astro-ph/9605155, UH-IFA-96-28 preprint, 16pp., to appear in *Relativistic Astrophysics: A Conference in Honor of Igor Novikov's 60th Birthday*, eds. B. Jones and D. Markovic for a more recent review and a collection of references.
- [17] A. Albrecht, P. Steinhardt, M. Turner, and F. Wilczek, Phys. Rev. Lett. **48**, 1437 (1982); A. Dolgov and A. Linde, Phys. Lett. **116B**, 329 (1982); L. Abbott, E. Farhi, Wise, Phys. Lett. **117B**, 29 (1982); D. Nanopoulos, K. Olive, and M. Srednicki, Phys. Lett. **127B**, 30 (1983); M. Morikawa and M. Sasaki, Prog. Theor. Phys. **72**, 782 (1984); A. Hosoya and M. Sakagami, Phys. Rev. D **29**, 2228 (1984).
- [18] Ivaylo Zlatev, Greg Huey, and Paul J. Steinhardt, Phys. Rev. D **57**, 2152 (1998).
- [19] E. Berezin and C. Itzykson, Phys. Rev. D **2**, 1191 (1970).
- [20] For a review, see M. Dine, *Supersymmetry phenomenology*, hep-ph/9612389 and refs. therein; G.F. Giudice and R. Rattazzi, *Theories with gauge mediated supersymmetry breaking*, hep-ph/9801271.
- [21] T. Han, T. Yanagida, and R.J. Zhang, hep-ph/9804228.
- [22] S. Raby, Phys. Rev. D **56**, 2852 (1997).
- [23] A. Riotto, hep-ph/9707330, to appear in Nucl. Phys. **B**.
- [24] K. Hamaguchi, Y. Nomura and T. Yanagida, hep-ph/9805346.
- [25] K. Benakli, J. Ellis, and D.V. Nanopoulos, hep-ph/9803333.

- [26] E. Kolb and M. Turner, *The Early Universe* (Addison-Wesley, Redwood City, CA, 1990); A. Linde, *Particle Physics and Inflationary Cosmology* (Harwood, Chur, Switzerland, 1990).
- [27] T. S. Bunch, *J. Phys.* **A 13**, 1297 (1980); L. Parker and S. A. Fulling, *Phys. Rev. D* **9**, 341 (1974); L. Parker, *Phys. Rev.* **183**, 1057 (1969).
- [28] N. D. Birrell and P. C. W. Davies, *Quantum Fields in Curved Space* (Cambridge University Press, Cambridge, 1982).
- [29] S. Fulling, *Gen. Rel. and Grav.* **10**, 807 (1979).
- [30] J. Audretsch and G. Schaefer, *Phys. Lett.* **66A**, 459 (1978).
- [31] C. Bernard and A. Duncan, *Ann. Phys.* **107**, 201 (1977).
- [32] D. Lyth and A. Riotto, hep-ph/9807278.
- [33] A. de Rújula, S. L. Glashow, and U. Sarid, *Nucl. Phys.* **B333**, 173 (1990).
- [34] J. L. Basdevant *et al.*, *Phys. Lett.* **234B**, 395 (1990).
- [35] G. Starkman, A. Gould, R. Esmilzadeh, and S. Dimopoulos, *Phys. Rev. D* **41**, 3594 (1990); D. O. Caldwell, *J. Phys. G***17**, S325 (1991).
- [36] G.D. Kribs and I.Z. Rothstein, *Phys. Rev. D* **55**, 4435 (1997).
- [37] V. A. Kuzmin and V. A. Rubakov, astro-ph/9709187.
- [38] V. Berezhinsky, M. Kachelriess, and A. Vilenkin, *Phys. Rev. Lett.* **79**, 4302 (1997).
- [39] R. N. Mohapatra and S. Nussinov, *Phys. Rev. D* **57**, 1940 (1998).
- [40] G. Jungman, M. Kamionkowski, and K. Griest, *Phys. Reports* **267**, 195 (1996).

APPENDIX

In this appendix we remind the reader of the boundary conditions for the classical fields (i.e. Eq. (10) and Eq. (11)) which is solved numerically. As we mentioned earlier, we will choose the initial conditions as to set up a slow-roll, large-field inflationary epoch, at the end of which the particle creation will occur. To gain intuition for the needed initial conditions, consider the slow-roll scenario as presented in [26]. From the Friedmann equation,

$$H \approx \sqrt{\frac{8\pi}{3M_{\text{Pl}}^2} \frac{\sqrt{V(\phi)}}{M_{\text{Pl}}}} \quad (\text{A1})$$

where $\dot{\phi}^2 \ll V(\phi)$ has been assumed (slow-roll scenario) and $V(\phi)$ is the inflaton potential. Since in general $\ddot{\phi} \ll 3H\dot{\phi}$ is required for sufficient inflation to occur, we can write

$$3H\dot{\phi} \approx -V(\phi)_{,\phi}. \quad (\text{A2})$$

Combining this with Eq. (A1) gives

$$a \approx a(t_p) \exp\left(\frac{-8\pi}{M_{\text{Pl}}^2} \int_{\phi(t_p)}^{\phi(t)} \frac{V(\phi)}{V_{,\phi}(\phi)} d\phi\right) \quad (\text{A3})$$

where t_p (p stands for past) is the time at the beginning of inflation. Hence, for potentials of the form constant $\times \phi^n$, the number of e-folds of inflation is determined solely by the initial and the final values of ϕ .

The end of the slow-roll scenario is obtained by determining when the potential energy of the inflaton becomes comparable to the kinetic energy. Eq. (A1) and Eq. (A2) combine to give (in addition to Eq. (A3))

$$\dot{\phi} = -\frac{M_{\text{Pl}} V_{,\phi}}{\sqrt{24\pi} \sqrt{V(\phi)}}. \quad (\text{A4})$$

which when combined with the approximate condition for the end of inflation (namely $\dot{\phi}^2/2 \approx V(\phi)$), we have

$$\frac{V(\phi(t_e))}{V_{,\phi}(\phi(t_e))} \approx \frac{M_{\text{Pl}}}{\sqrt{48\pi}} \quad (\text{A5})$$

where t_e is the time at the end of inflation.

Therefore, for potentials of the form constant $\times \phi^n$, fixing the number of e-folds fixes the initial value. For $V(\phi) = m_\phi^2 \phi^2/2$ potential, we thus have

$$\phi(t_e) \approx M_{\text{Pl}}/\sqrt{12\pi} \quad (\text{A6})$$

and

$$\phi(t_p) \approx \frac{M_{\text{Pl}}}{\sqrt{2\pi}} \sqrt{N_e + 1/6} \quad (\text{A7})$$

where N_e is the number of inflationary e-folds. For our typical runs, we use $N_e \approx 64$. Then Eq. (A4) (equivalent to assuming $\ddot{\phi} = 0$) gives the initial condition for $\dot{\phi}$.

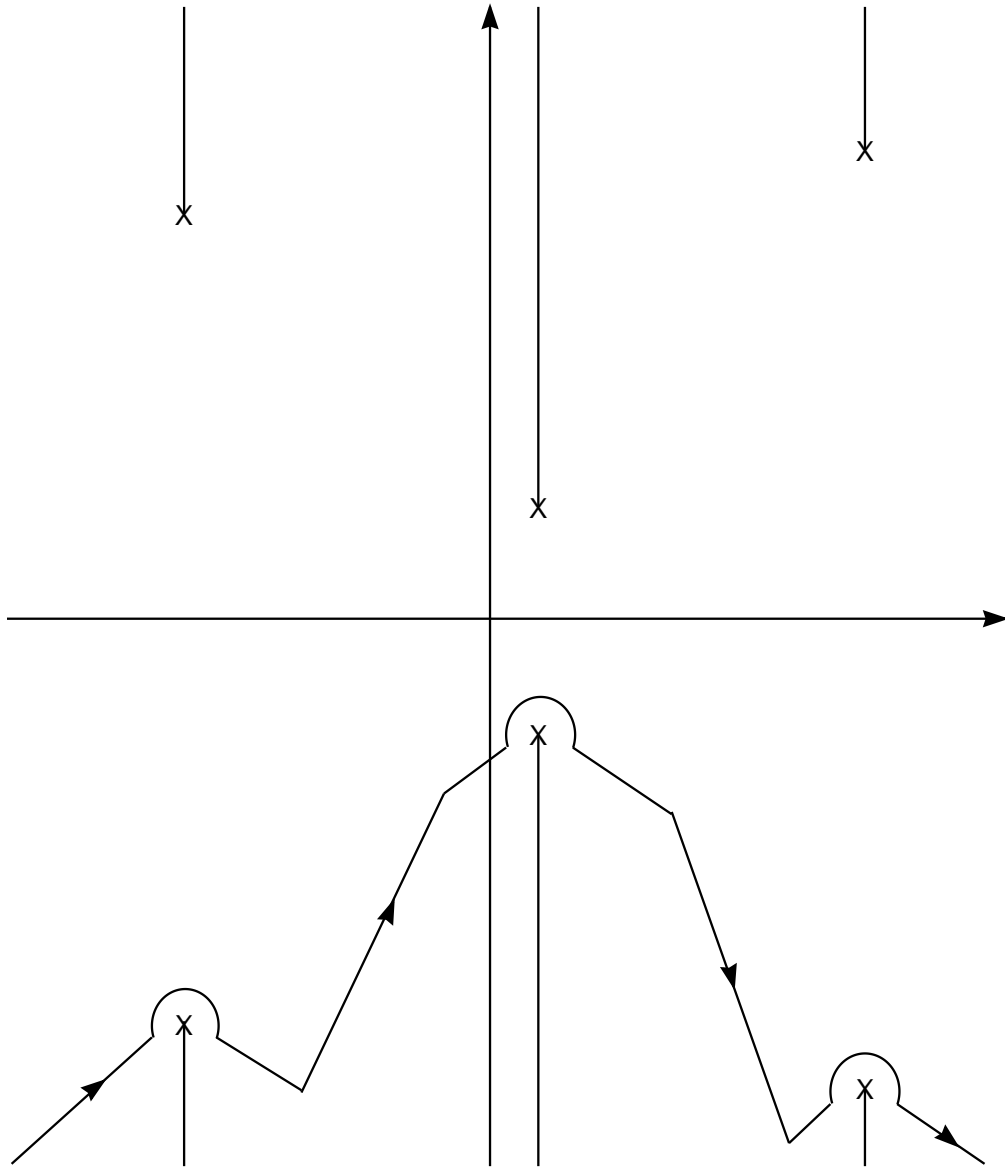


Figure 1: A schematic sketch of the analytic structure of Eq. (21) on the complex η plane is shown. The crosses represent branch points and the lines emanating from them branch cuts. Shown also is a schematic sketch of the appropriately deformed contour for the steepest descent approximation on the lower half plane.

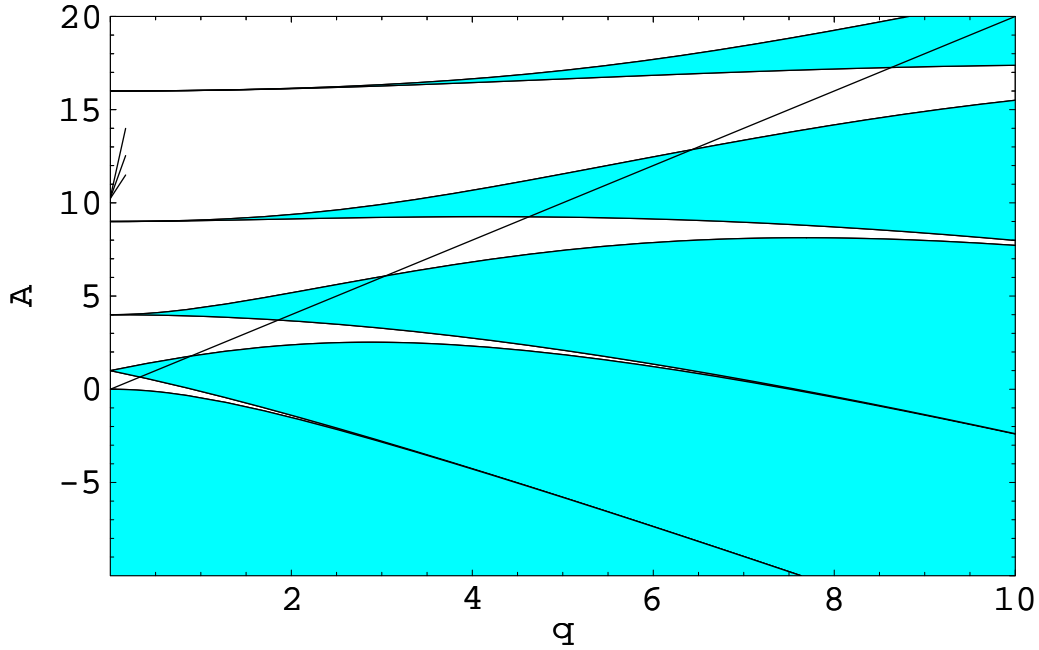


Figure 2: Shown is the Mathieu instability chart. For the values of A and q that fall in the shaded region, the solution to the Mathieu equation is unstable. The line connecting the origin to the upper right corner of the plot is $A = 2q$. All A and q trajectories must lie above this line by their definition in Eq. (67). The three short line segments near $(q, A) = (0, 11)$ represents three representative trajectories each having different values of k (for those k values that dominate the number density integral) for $gM_{\text{Pl}}/H_i = 45$ and $b = 7$. Although none of the trajectories cross any of the instability bands, there is an enhancement by a factor 100 in the particle density production.

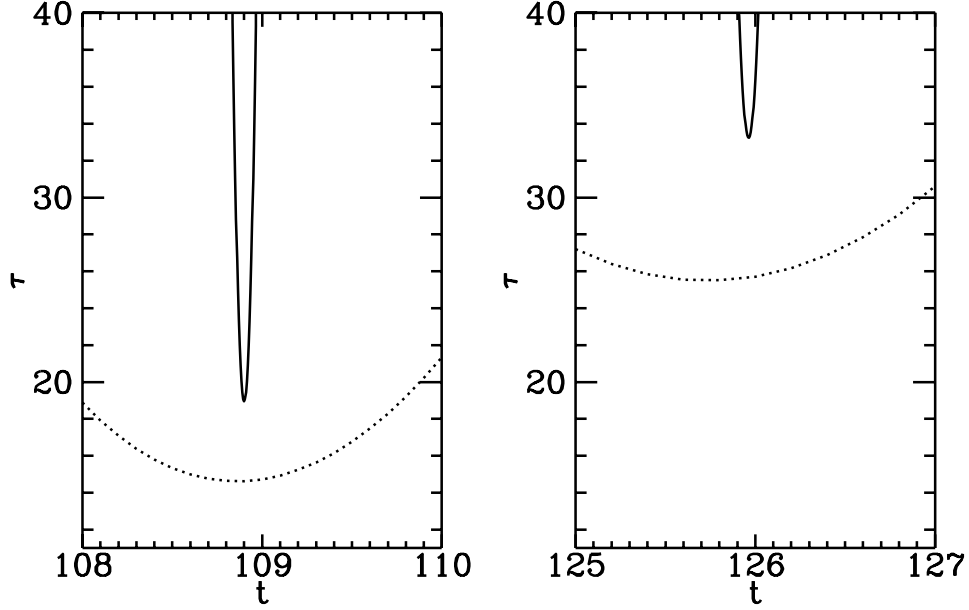


Figure 3: Here we plot the number density suppressing exponent $\tau \equiv 4b/(H_{\text{eff}}^2(t) + R_{\text{eff}}(t)/6)^{1/2}$ as a function of t (in units of $\sim 1/(12.2H_i)$) near the values corresponding to the conformal time r which solves Eqs. (37) and (38). The solid curve corresponds to the case $b = 1080$ and $gM_{\text{Pl}}/H_i = 10^6$. The dotted curve corresponds to $b = 30$ and $g = 10^3$. The actual values of r solving Eqs. (37) and (38) with these parameters lie very close to the minimum of these curves (there exists only one solution r per curve shown). Exact numerical value examples are given in the text. The $t(r)$ near 109 and near 126 gives the smallest two τ values for each parameter set. Clearly the pole having a real part r with $t(r)$ near 109 dominates.

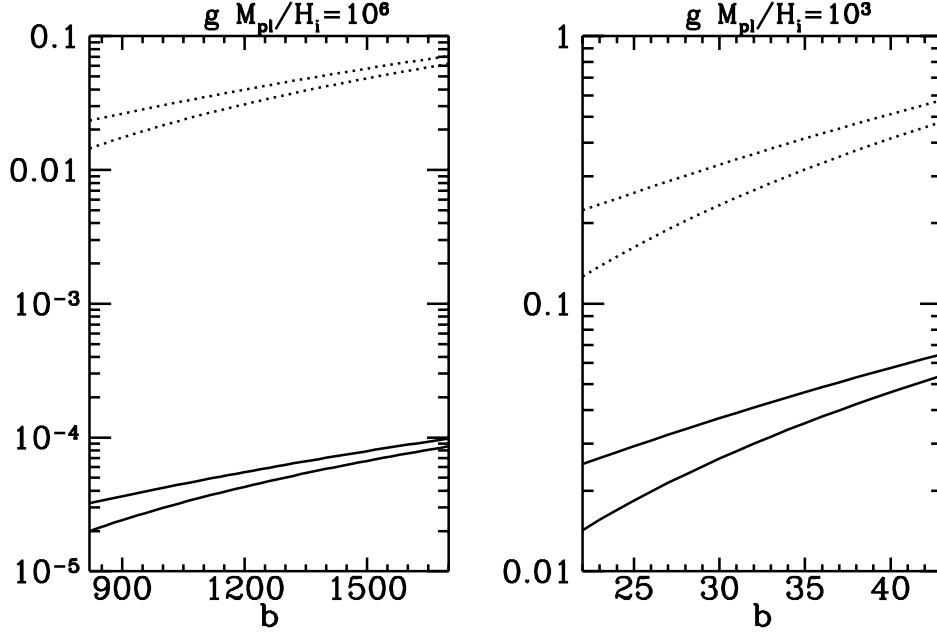


Figure 4: We plot as a function of $b \equiv M_X/H_i$ the quantities that must be less than unity for the Taylor series truncation to be valid. The solid curves correspond to the left hand side of Eq. (40), and the dotted curves correspond to the left hand side of Eq. (39). The lower of the given curve type corresponds to $k/(a_i H_i) = 0$. The upper of the given curve type corresponds to $k/(a_i H_i) = 1000$ for the $gM_{\text{Pl}}/H_i = 10^6$ case and $k/(a_i H_i) = 30$ for the $gM_{\text{Pl}}/H_i = 10^3$ case. These k values indicate the momentum range over which the particles are produced. The expansion truncation is clearly justified in the $gM_{\text{Pl}}/H_i = 10^6$ case while it is marginally adequate in the $gM_{\text{Pl}}/H_i = 10^3$ case.

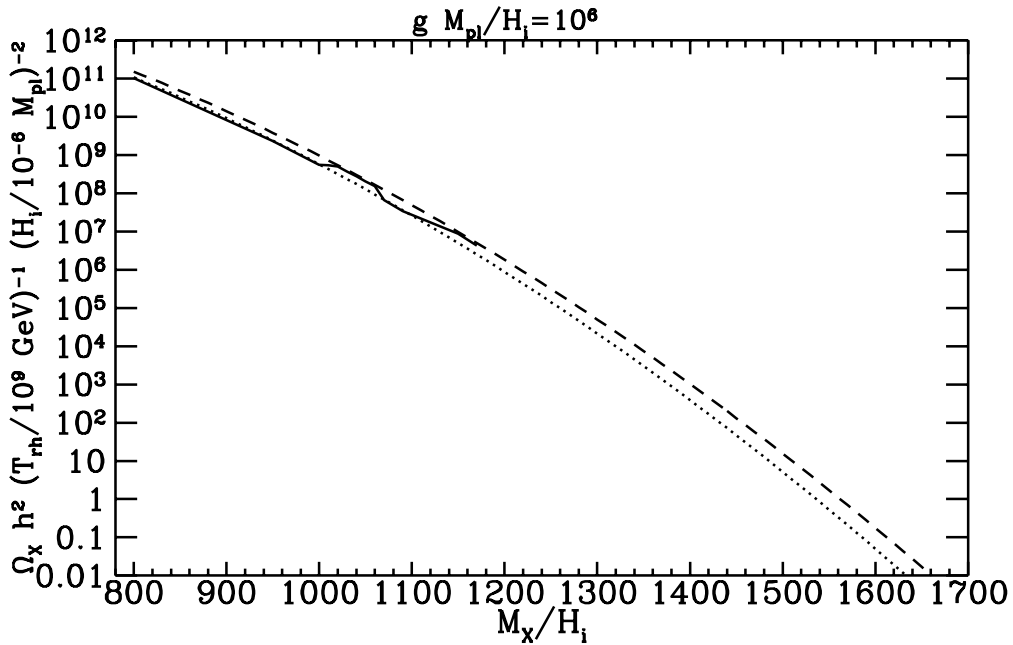


Figure 5: The solid curve in this plot of $\Omega_X h^2/S$ versus b for $gM_{\text{Pl}}/H_i = 10^6$ shows the numerical results. The correction factor (explained in the text) used for the dotted curve is 0.932 and for the dashed curve is 0.903. Hence, unless if $H_i > 10^{-6} M_{\text{Pl}}$ or $T_{\text{RH}} > 10^9$ GeV, cosmologically significant dark matter production in this scenario does not occur for masses above about $1700H_i$, which can be in the GUT scale.

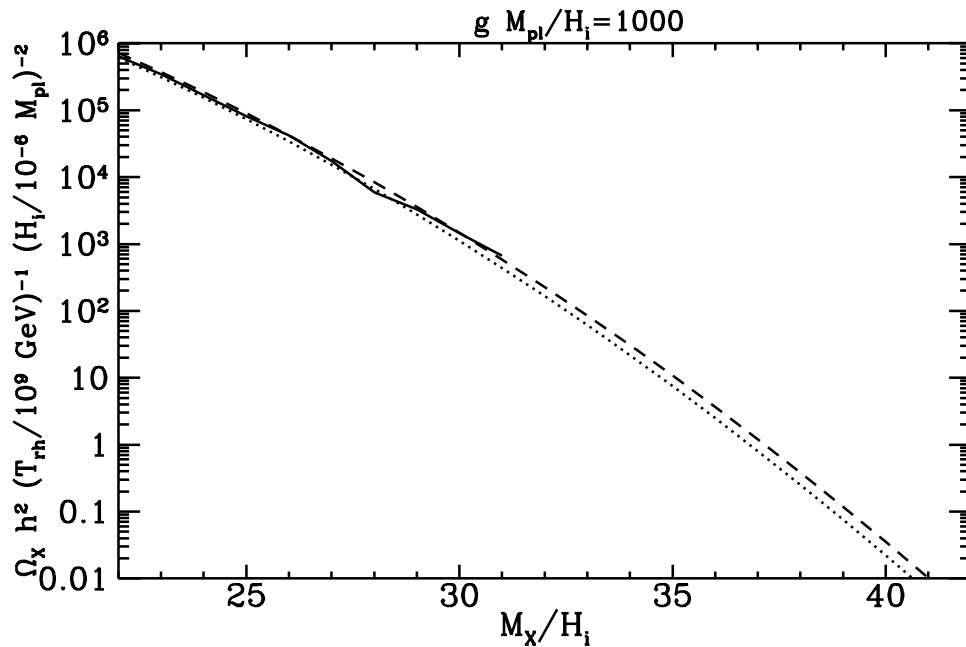


Figure 6: The solid curve in this plot of $\Omega_X h^2/S$ versus b for $gM_{\text{Pl}}/H_i = 10^3$ shows the numerical results. The correction factor (explained in the text) used for the dotted curve is 0.98 and for the dashed curve is 0.963, both of which are quite close to the values used in Fig. 5. Hence, we see that our analytic approximation seems to be in agreement with the numerical results.

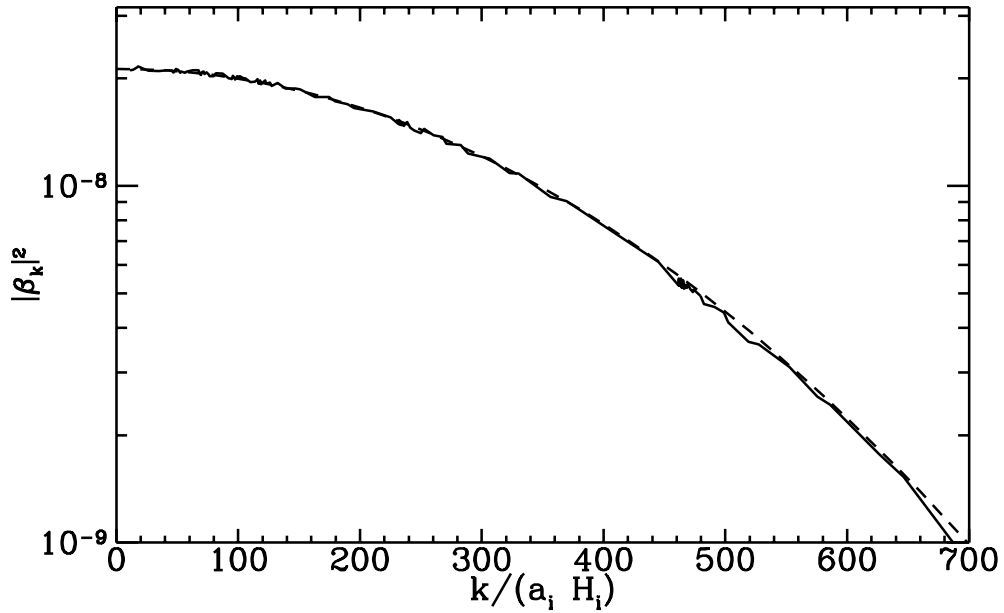


Figure 7: For the parameters $gM_{\text{Pl}}/H_i = 10^6$ and $b = 1080$, the particle density per mode is plotted as a function of the wave vector scaled by the scale factor a_i and the Hubble expansion rate H_i at the end of inflation. The solid curve corresponds to the the brute force numerical results. The dashed curve corresponds to the spectrum obtained using the analytic approximation Eq. (69) with $f = 0.932$.

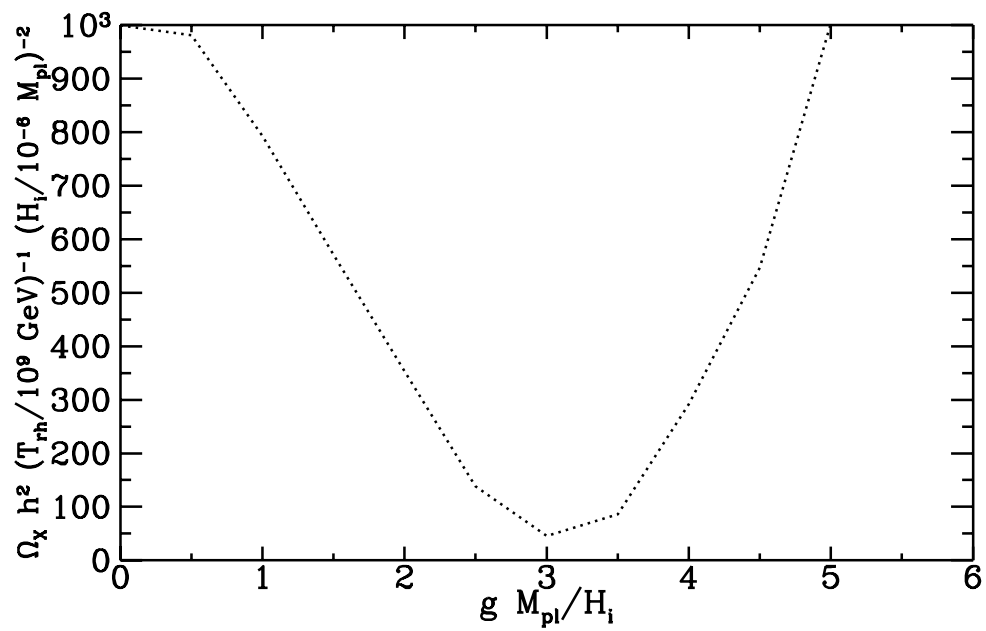


Figure 8: The plot shows the nonmonotonic behavior of the particle density produced with the variation of the coupling constant. The value of $b \equiv M_X/H_i$ is set to 1 here.